Development and characterization of polymeric microparticle of poly(D,L-lactic acid) loaded with holmium acetylacetonate

Article *in* Journal of Microencapsulation · May 2018

DOI: 10.1080/02652048.2018.1477843

Caio Barros
University College Dublin

Ljubica Tasic
University of Campinas

Journal of Microencapsulation
Micro and Nano Carriers

ISSN: 0265-2048 (Print) 1464-5246 (Online) Journal homepage: http://www.tandfonline.com/loi/imnc20

Development and characterization of polymeric microparticle of poly(D,L-lactic acid) loaded with holmium acetylacetonate

Mariangela de Burgos M. de Azevedo, Vitor H. S. de Melo, Carlos Roberto J. Soares, Douglas M. Miyamoto, Ricardo A. Katayama, Peterson L. Squair, Caio H. N. Barros & Ljubica Tasic

To cite this article: Mariangela de Burgos M. de Azevedo, Vitor H. S. de Melo, Carlos Roberto J. Soares, Douglas M. Miyamoto, Ricardo A. Katayama, Peterson L. Squair, Caio H. N. Barros & Ljubica Tasic (2018): Development and characterization of polymeric microparticle of poly(D,L-lactic acid) loaded with holmium acetylacetonate, Journal of Microencapsulation, DOI: 10.1080/02652048.2018.1477843

To link to this article: https://doi.org/10.1080/02652048.2018.1477843

Development and characterization of polymeric microparticle of poly(D,L-lactic acid) loaded with holmium acetylacetonate

Mariangela de Burgos M. de Azevedo[1,2], Vitor H. S. de Melo[1], Carlos Roberto J. Soares[1], Douglas M. Miyamoto[1]; Ricardo A. Katayama[1], Peterson L. Squair[1], Caio H. N. Barros[3], Ljubica Tasic[3].

[1] *Instituto de Pesquisas Energéticas e Nucleares (IPEN/CNEN-SP);*
[2] *Centro de Biotecnologia da Amazônia - CBA- Manaus - AM.*
[3] *Instituto de Química, Departamento de Química Orgânica, UNICAMP, SP.*

E-mail:mariangela.burgos@pq.cnpq.br

Development and characterization of polymeric microparticle of poly(D,L-lactic acid) loaded with holmium acetylacetonate

Biodegradable polymers containing radioactive isotopes such as Holmium 166 (^{166}Ho) have potential applications as beta particle emitters in tumor tissues. It is also a gamma ray emitter, allowing nuclear imaging of any tissue to be acquired. It is frequently used in the form of complexes such as holmium acetylacetonate (HoAcAc), which may cause damages in tissues next to the targets cancer cells, as it is difficult to control its linkage or healthy tissues radiotherapy effects. Poly(D,L-lactic acid), PDLLA, was used to encapsulate holmium acetylacetonate (HoAcAc) using an emulsion solvent extraction/evaporation technique. Microspheres with sizes between 20-53 μm were extensively characterized. HoAcAc release from the microspheres was assessed through studies using Inductively Coupled Plasma – Optical Emission Spectroscopy, and the microspheres showed no holmium leakage after a period of 10 half-lives and following gamma irradiation. Thus, HoAcAc loaded microspheres are here presented as a potential system for brachytherapy and imaging purposes.

Keywords: PDLLA, holmium acetylcetonate, brachytherapy, microspheres

Introduction

The large variety of particles, techniques, and treated tumors in the studies provided an important insight into issues concerning efficacy, safety, particle and isotope choice, and other concepts for future research (Bakker *et al*. 2017).

Prognosis of hepatic cancers - which quickly tend to originate metastasis in new organs (Dhanasekahan *et al*. 2012) has led to many strategies towards the development of new radiotherapy modalities. These techniques avoid totally or partially the injuries in healthy tissues caused by the absorption of toxic substances, or side effects related to the passage of a radioactive particle beam - even by release of auger electrons (Milenic *et al*. 2004). The intra-arterial administration of radioactive particles through a catheter into vases directed to the liver is a new modality, also called hepatic brachytherapy or radioembolization. Such particles are tumor-directed radiation delivery systems, limiting the escape rate of radioisotopes to neighboring healthy organs. The possibility of delivering higher doses of radiation may eliminate tumors in a short time of repeated procedures. Moreover, loaded biodegradable microparticles with a fine-tuned size can block microcirculation (and nutrient supply) in tumor tissues. In order to design novel microparticles loaded with radionuclides, a few characteristics must be pursued, such as:

(1) resistance to the radionuclide activation (and possibly to gamma-rays sterilization procedure (Sato 1983); (2) chemical stability to prevent an earlier elution of radioactive substances; (3) low immunoreactivity (Frank and Fries 1991; Owens and Peppas 2006), and (4) narrow size distribution, suitable for the embolization, restricted to the organ of interest.

Beta emitter radioisotopes are widely used for radiotherapy purposes because of their suitable long path length and low linear energy transfer values. The beta particles penetrate tissues and interact with atoms, mainly from water, generating excited species, ionized atoms and/or free radicals that damage organelles and induce single and double strand breaks in DNA (Lliakis 1991). Holmium-166 is a promising radiopharmaceutical to be used in radiotherapy (and brachytherapy) procedures, for many reasons. Its beta emission (E_{max} = 1.85 MeV) may reach 2.3 mm in tissues (Kim *et al*. 2004) and the half-life of this rare earth element (26.8 h) is long enough for nuclear activation of finalized or stocked systems well as for proper delivery of higher doses of radiation. The energy of the holmium gamma emission ($E_{\gamma med}$ = 80.6 keV (6.06%); $E_{\gamma max}$ = 1.38 MeV, (0.93%)) (Rajendran *et al*. 2002; Tuner *et al*. 1994) penetrates the human body and allows scintigraphy diagnostics (Nijsen *et al*. 1999; Zielhuis *et al*. 2007; Vente *et al*. 2008). The naturally found holmium is monoisotopic, which turns its activation into a simple process that may be carried out in the Research Nuclear Reactor IEA-R1 (IPEN, Sao Paulo, Brazil). Ho^{+3} is paramagnetic, thus its compounds are promising as contrast agents for image acquisition by Nuclear Magnetic Resonance medical equipment (Speenwoolde et al., 2004). However, despite the low toxicity (50-500 mg kg^{-1} bodyweight), it is known that rare earth elements accumulate in bones (Thunus and Lejeune 1999); hence, they should be retained inside non-absorbable compounds or matrixes while they maintain their radioactive properties, and their preferable release should be in the form of stable coordination compounds.

A restriction to intra-arterial administration of microparticles is their elimination by human metabolism. The leaking of these microspheres to other organs may induce an undesirable embolization, rupture of vessels and even hemorrhage. Biodegradable and biocompatible materials are proposed as a matrix for radioisotope loaded particles due to the perspective of a short time existence, decreasing the possibility of embolization.

The most studied biodegradable material is the poly(lactic acid), PLA. This polyester can be prepared as dextrogirous (PDLA), levogirous (PLLA), racemic

(PDLLA) and meso (an equimolar mixture of the PDLA and PLLA) (Jacobsen *et al*. 1999; Han *et al*. 2001; Garlotta 2001; Kricheldorf 2001; Seyednejad *et al*. 2001; Södergård and Stolt 2002; Avinc and Khoddami 2009; Cheng *et al*. 2009;). PLAs are very promising for pharmaceutical and biomedical aims in drug delivery systems and for tissue engineering purposes (Spinu *et al*. 1996; Ikada and Tsuji 2000; Dubois and Narayan 2003; Cui *et al*. 2007; Helen and Gough 2008; Jain *et al*. 2010; Xu *et al*. 2011; Leal *et al*. 2015).

Holmium acetylacetonate loaded PLLA microspheres are often cited as promising radiopharmaceuticals for hepatic cancer brachytherapy (Lliakis 1991; Mumper and Jay 1991; Nijsen *et al*. 2001; Van Es *et al*. 2001; Nijsen *et al*. 2002; Rajendran *et al*. 2002; Zielhuis *et al*. 2006; Costa *et al*. 2009; Smits *et al*. 2010). Acetylacetonate complexes are known for their stability, providing suitable retention of the rare earth ion in biological systems. As these complexes are smaller, they are easily eliminated by the human metabolism. On the other hand, PLLA's higher degree of crystallinity induces a disadvantageous slower degradation under biological conditions (Hu *et al*. 2001). Among the PLAs recently investigated by some authors of the present manuscript (Costa *et al*. 2009; Piovan *et al*. 2011), the racemic mixture PDLLA showed to be an alternative substitute matrix to particulate radiopharmaceuticals due to the following reasons: (1) it is cheaper when compared to PLLA, (2) reduced crystallinity, since it is a racemic material (Avinc and Khoddami 2009) and (3) good biocompatibility with human cells (Lin *et al*. 2006). Additionally, coexistence of D and L lactic acid monomers gives PDLLA better thermoplastic properties and might facilitate industrial processing (due to its lower melting point) and under certain conditions it can be degraded non-enzymatically. The degree of crystallinity and other properties of this racemic polyester are controlled by enantiomeric ratio and the type of catalyst used in preparation (Avinc and Khoddami 2009).

The aim of this study is the production and characterization of PDLLA microspheres (MS-PDLLA) loaded with holmium acetylacetonate (HoAcAc) for the treatment of hepatic cancer via brachytherapy through the emission of beta radiation. In addition to this application, considering the emission of gamma rays by ^{165}Ho, the microspheres can be used for tissue nuclear imaging purposes. MS-PDLLA and HoAcAc loaded PDLLA microspheres (MS-PDLLA-HoAcAc) were evaluated by Differential Thermal Analysis (DTA), Thermogravimetry Analysis (TGA), Scanning Electron Microscopy (SEM), Energy Dispersive X-Ray Detector (EDS), Fourier Transform Infrared Spectroscopy (FTIR) and Laser Optical Microscopy. A gamma irradiated MS-PDLLA-HoAcAc sample was analyzed by SEM, and the release of a complex of microparticles in phosphate buffer pH 7.4 was assessed by Inductively Coupled Plasma – Optical Emission Spectroscopy (ICP-OES).

Materials and methods

PDLLA (M_w 75,000-120,000, inherent viscosity 0.55-0.75 dL g^{-1}, melting point of 262 °C, glass transition temperature of 32.9 °C), acetylacetone, holmium III chloride hexahydrate, and poly(vinyl alcohol) (PVA) 98-99% hydrolyzed (M_w 31,000-50,000) were obtained from Sigma Aldrich.

Synthesis of HoAcAc, MS-PDLLA and MS-PDLLA-HoAcAc

Raw tri-hydrated HoAcAc was prepared by an adapted method of Nijsen *et al*. (1999). Acetylacetone (180 g) was dissolved in 1.0 L of water and the pH was brought to 8.52 with NH_4OH. Holmium chloride (10 g dissolved in 30 mL of water) was added into this solution. HoAcAc crystals were formed at room temperature after 24 h; the crystals were then collected by simple filtration, washed exhaustively with water, and dried in a vacuum oven.

MS-PDLLA and MS-PDLLA-HoAcAc were prepared by the emulsion solvent extraction/evaporation technique. PDLLA (1.2 g) or PDLLA (1.2 g) and HoAcAc (1.2 g), were dissolved in chloroform (38 mL) and, under stirring speed of 800 rpm, the organic solution was emulsified in 200 mL of water with PVA 2% (w/w), for 21 h. During this period, the organic solvent was evaporated from the system. The solid microspheres (MS) were collected and washed by centrifugation using ultrapure water, 0.1 mol L^{-1} HCl, and ultrapure water again. Finally, MS-PDLLA and MS-PDLLA-HoAcAc were suspended in ultrapure water and fractionated in stainless steel sieves to isolate those with sizes between 20-53 µm (ideal for hepatic brachytherapy purposes). The samples were then freeze-dried.

Thermogravimetric analysis (TGA)

Thermogravimetric analysis (TGA) was carried out using a Universal V4.5A TA Instruments, model 2950 TGA HR V5.4A, under nitrogen atmosphere (10-50 mL min^{-1}), at heating rate of 10 °C min^{-1}. Differential Thermogravimetric Analysis (DTA) was performed in a TGA-DTA Netzsch STA 409 C/CD, under argonium atmosphere (1 mL min^{-1}) and heating rate of 15 K min^{-1}. For both TGA and DTA analyses, the temperature ranges were of 25-900 °C.

Scanning Electron Microscopy (SEM)

Scanning Electron Microscopy (SEM) images were obtained in a Phillips XL 30 Microscope and JEOL model JSM-7401, with operating voltage of 1.0 kV, and carbon-covered samples in a Sputter Coater BAL-TEC SCD 050; or in a Hitachi Analytical Table Top Microscope TM3000 with Energy Dispersive X-Ray Detector (EDS), 15 kV operating voltage (Analytical mode).

FTIR analysis

Fourier-Transform Infrared Spectroscopy (FTIR) was performed in a Nicolet 6700 FTIR spectrometer equipped with ATR and BOMEM MB-100 Economical High Performance FTIR. Samples were previously, dried at 100 °C, for 48 h; 1-2 mg of material was mixed in 100 mg of KBr to form a pellet. Spectra were measured in transmittance, wavenumber range from 4000 to 400 cm^{-1}.

Fluorescence imaging

Fluorescence images were obtained in a Zeiss Axioscop 40 HBO 50/AC Optical Microscope using a 450-490 nm filter for excitation, and monitoring fluoresce emission at 515 nm. The magnification used was 20x.

Gamma irradiation

The gamma irradiation technique was performed in a Gamma cell IPEN/CNEN-SP, using a ^{60}Co source, to reach a 25 kGy dose, with dose rate of 1.69 kGy h^{-1} (Piovan *et al*. 2011).

ICP-OES analysis

Inductively Coupled Plasma – Optical Emission Spectroscopy (ICP-OES) was performed in inorganic determinations of low concentrations of the target trace elements, with high sensitivity. ICP-OES Varian Inc. has axially viewed plasma, concentric glass nebulizer and megapixel CCD detector. Argon was used as the plasma and auxiliary gas. The optical system was thermally stabilized, containing no moving parts to ensure long-term stability. The plasma needed to be turned on 30 min prior to the analysis for stabilization.

Holmium release studies

For simulations of holmium complex release in physiological medium, a sample of 10.0 mg of MS-PDLLA-HoAcAc SI was left in 50 mL of phosphate buffer saline (PBS, pH 7.40) to simulate the release of the holmium complex in the simplest environment representing a physiological condition. The period of study was 11 days, corresponding to 10 half-lives of the holmium-166 decay.

Results and discussion

Several preparation methods are described for the use of PLA or PLGA (poly(lactic-co-glycolic acid) polymers, among which the emulsion-solvent evaporation, phase separation, spray drying, supercritical fluid, and membrane emulsification methods are commonly used in practice (Han *et al*. 2016). In this work, we chose the Emulsion-solvent evaporation method, an easy process to produce the well-formed microparticles which are and suitable for small scales, this is the most described method for preparation of PLA and PLGA microspheres (Yang and Chi 2000; Rosca *et al*. 2004).

In the Phase Separation Method, the drugs and emulsion droplets are, firstly, dispersed in the PLGA solvent, forming condensation nuclei, and the new phase (the condensed phase) is formed after polycoagulant be dropped into the solvent. The solubility of the solvent is reduced and precipitates on the surfaces of the condensation nuclei (Mi *et al*. 2002). Fine spherical microparticles may be obtained by repeating the processes of precipitation, dissolution, and precipitation while the mixture was stirred. The current problem with this method is that a large amount of organic solvent should be used as the polycoagulant, which cannot be removed from the final product, causing toxicity, environmental pollution, and residues of organic solvent.

In the Spray drying method, polymers are dissolved in a low-boiling-point solvent, into which the granulated drug is mixed. The polymer solution is, then, sprayed from a nebulizer and dried by up-flowing nitrogen gas, forming microspheres. This method is suitable for preparing drugs, albumin, and peptide embedded microspheres on a large scale or for industrial purposes (Jain 2001; Giunchedi *et al*. 2001).

The Supercritical fluid method has been widely used to prepare drug carriers, and it has the advantages of a less residual solvent, mild reaction and short period of time required.

The method has been used to either implant insoluble drugs into nanoparticles or to embed drugs in polymers, and drug-loaded microspheres with a core–shell structure may be manufactured, allowing controlled drug release (Williams *et al*. 2002; Jung and Perrut 2001; Ginty *et al*. 2005).

The Membrane emulsification method involves the imposition of an external pressure on a discrete phase, causing permeating on inorganic membrane to obtain a continuous phase. Uniform microspheres were obtained by controlling the pressure and membrane bore diameter (Shiga *et al*. 1996; Gasparini *et al*. 2008). Compared with traditional methods, such as emulsion solvent evaporation method, this method was suitable for the large-scale manufacturing of microspheres.

SEM, EDS and Optical Microscopy

SEM images of MS-PDLLA and MS-PDLLA-HoAcAc (Figure 1(A,B)) revealed distinct morphologies. The unloaded polymeric microspheres are spherical and have a smooth surface. However, the solid loaded microspheres (with sizes between 20-53 μm) present a rather rough topography with small, well-spaced round structures on their surface. The MS-PDLLA-HoAcAc tolerate the gamma rays of 25 kGy, which is proposed as form of sterilizing materials (as seen in Figure 1 (C,D). The emulsion solvent extraction/evaporation technique of synthesis of solid microspheres presents the advantages of being a low cost chemical method that is suitable for the production of microparticles in the desirable size range for hepatic brachytherapy purposes. Nevertheless, the method of co-axial electrohydrodynamic atomization (EDHA) has emerged as a one-step process for the synthesis of polymer nano- and microparticles especially when smaller sizes and narrower size distributions are desired (for instance, for the delivery of anticancer drugs) (Parhizkar *et al*. 2016; Reardon *et al*. 2017; Shams *et al*. 2017). Therefore, the choice of the method to be used in the preparation of microspheres is directly related to the end use of these particles.

FIGURE 1

The fluorescence emission image of MS-PDLLA-HoAcAc showed typical green fluorescence of holmium III (Figure 2(A)), related to its strongest luminescent decay in the visible spectra involving the electronic transition $^5S_2$ $^5I_8$ (Bunzli and Piguet, 2005). Based on this, a SEM micrograph of raw HoAcAc (Figure 2(B)) was acquired. Elongated and shiny crystals are morphologically quite consistent as to the aspect of bright spikes in the MS-PDLLA-HoAcAc (Figure 1(B)). Finally, the EDS spectra of MS-PDLLA-HoAcAc showed peaks of holmium (Figure 2(C)). Therefore, the results indicate a complex loading in polyester matrix, which agree with the morphological differences between MS-PDLLA-HoAcAc and MS-PDLLA. Loading with more than 12% of HoAcAc (Nijsen *et al*. 2001) is considered optimal, so it was estimated that MS-PDLLA-HoAcAc have a higher amount of the complex, given the thermogravimetric data which are explained in the following sections.

FIGURE 2

FTIR Spectra

Comparative FTIR spectra of the raw complex, the emulsifying agent, and the microspheres are shown in Figure 3 and the assignment of their normal modes is reported in Table 1. According to the literature data (Colthulp *et al*. 1990; Kaitia *et al*. 1996; Diaz-

Acosta *et al*. 2001; Mansur *et al*. 2008), the HoAcAc normal modes at 1605 cm^{-1} and 1524 cm^{-1} reveal coordination of acetylacetonate ligands to the Ho^{+3} by its enol tautomer and the broad band at 3421 cm^{-1} corresponds to the inner sphere and hydration water molecules. An interesting property was revealed by the split of ν(Ho-O) into two bands at 494 cm^{-1} and 474 cm^{-1}, suggesting that the acetylacetonates are bonded to Ho^{+3} unequally. The most uncommon normal mode is the π(C-H), at 698 cm^{-1} and 764 cm^{-1}. Their attribution based on acetylacetonate transition metal complexes (Diaz-Acosta *et al*. 2001) is “in plane deformation ring mode”, which means that chemical bonds of Ho^{+3} and bidentate enol tautomer of acetylacetonate may define electronic delocalized systems resembling aromatic rings.

FIGURE 3

TABLE 1

The PVA spectrum presents characteristic bands in the range of 3200-3550 cm^{-1} related to the stretching modeν(O-H) and at 916 cm^{-1} and 848 cm^{-1}, which are typical of their isotactic and syndiotactic sequences, respectively (Mansur *et al*. 2008). It can be stated that the MS-PDLLA and MS-PDLLA-HoAcAc had a non-expressive incorporation of the emulsifying agent, once there are no exclusive PVA vibrational bands in the MS infrared spectra.

The MS-PDLLA-HoAcAc FTIR spectrum presents well-defined normal modes typical of HoAcAc, which confirms the information obtained by optical microscopy, SEM and EDS. The fact that the MS-PDLLA-HoAcAc spectrum contains sharper polymer normal modes than those in the MS-PDLLA spectrum indicates that a high amount of complex crystals may enhance the packing of polyester. A possible mechanism for this effect is the replacement of labile inner sphere water molecules by the PDLLA carbonyl groups. In this case, a new crystallization pattern of PDLLA in the MS-PDLLA-HoAcAc is expected, which agrees with the morphological differences verified in the SEM micrographs.

TGA and DTA

A model for HoAcAc degradation was proposed based on the one proposed by Hussein *et al*. (1995) and Hussein *et al*. (1996) applied to lanthanum acetylacetonate ($La(acac)_3$), which presents many stages of thermal decomposition under N_2 atmosphere.

Three stages of propyne elimination are considered by the analogy with the lanthanum acetylacetonate case (Equations III, IV and V).

Release of hydration water molecules
$Ho(acac)_3.3H_2O$ $Ho(acac)_3.2H_2O$ (I)
[498.29 gmol^{-1}/516.30 gmol^{-1}].100% = 96.51%
↓
Release of inner sphere water molecules
$Ho(acac)_3.2H_2O$ $Ho(acac)_3$ (II)
[462.26 gmol^{-1}/516.30 gmol^{-1}].100% = 89.53%
↓
First propyne elimination
$Ho(acac)_3$ $Ho(CH_3COO)(acac)_2 + C_3H_4$ (III)
[422.19 gmol^{-1}/516.30 gmol^{-1}].100 % = 81.77%
↓
Second propyne elimination
$Ho(CH_3COO)(acac)_2$ $Ho(CH_3COO)_2(acac) + C_3H_4$ (IV)
[382.13 gmol^{-1}/516.30 g.mol^{-1}].100% = 74.01%
↓
Third propyne elimination and holmium acetate formation
$Ho(CH_3COO)_2(acac)$ $Ho(CH_3COO)_3 + C_3H_4$ (V)
[342.06 gmol^{-1}/516.30 gmol^{-1}].100% = 66.25%
↓
Holmium carbonate formation
$2Ho(CH_3COO)_3$ $Ho_2(CO_3)_3 + 3CH_3COCH_3$ (VI)
[509.89 gmol^{-1}/(2x516.30 gmol^{-1})].100% = 49.38%
↓

Holmium oxycarbonate formation
$Ho_2(CO_3)_3 \quad Ho_2O_2CO_3$ (VII)
[421.87 $gmol^{-1}$/(2x516.30 $gmol^{-1}$)].100% = 40.86%
↓
Holmium III oxide formation
$Ho_2O_2CO_3 \quad Ho_2O_3 + CO_2$ (VIII)
[377.86 $gmol^{-1}$/(2x516.30 $gmol^{-1}$)].100% = 36.59%

The intent of the TGA analysis was to characterize the thermal degradation process of HoAcAc and MS-PDLLA-HoAcAc. These results are presented in Figure 4.

FIGURE 4

After two events, considering the similar theoretical and experimental values (89.53% and 89.47%, respectively), the dehydration of the complex is proposed. However, the output order is 2 molecules of water in the first mass loss, occurring at 92.46 °C (Figure 4(A)) rather than one, as described by Koojiman *et al*. (2000). This assignment is based on the calculation according to HoAcAc with 1 and 3 water molecules in the minimal formula and molar masses of 480.27 $gmol^{-1}$ and 516.30 $gmol^{-1}$, respectively. This value is consistent with the experimental one, with a percentile residue of 93.08% in mass. Hence, it can be assumed that HoAcAc has probably one inner sphere water coordinated to Ho^{+3}, eliminated at 137.29 °C, during the second mass loss event. Considering the two energies of *v*(Ho-O) proposed in the analysis of HoAcAc FTIR spectrum, the arrangement of acetylacetonate ligands around the rare earth ion is asymmetric. Consequently, the elimination of propyne molecules is a multistep process.

Nevertheless, the first derivative of HoAcAc TGA curve lacks indication of thermal events related to individual outputs of first and second propyne molecules (third and fourth stages of proposed theoretical model). It was noted only the third event of mass loss in TGA curve, with residue of 74.21% in mass, similar to the theoretical percentage corresponding to HoAcAc, after a release of two propyne molecules (74.01%). Two acetylacetonates coordinated to Ho^{+3} define chemical bonds with closer relative stabilities, so their thermal events (such as degradation to acetate anion due to propyne release) occur at similar temperatures. Thus, a mixed salt is formed under the average temperature of 239.51 °C. Final release of propyne and conversion to holmium III acetate (step V of theoretical model, theoretical mass percentage of 66.25%) was noted only due to the change in the pattern of the first derivative, although partially hidden by the following colder thermal event. The last event has average temperature of 281.99 °C and it corresponds to the fourth thermal event in Figure 4(A), with an experimental mass percentage is 66.50%.

However, the fifth thermal event (average temperature of 400.02 °C) is unexpected according to the acetylacetonate lanthanum model. It was attributed as a mixed salt intermediate with the minimal formula of $Ho_2(CH_3COO)_4(CO_3)$ and molar mass of 626.05 gmol^{-1}. Such property again showed 2 acetates strongly linked to Ho^{+3}, which is consistent with the proposal of two initial acetylacetonates defining quite similar chemical bonds with the rare earth ion. Finally, a sixth event involves the mixed salt $Ho_2(CH_3COO)_4(CO_3)$ conversion into $Ho_2(CO_3)_3$. Based on experimental data, the theoretical model has been redesigned, and the following formulae are proposed:

$$[Ho(acac)_3(H_2O)].2H_2O \xrightarrow{92.5\,^{\circ}C} [Ho(acac)_3(H_2O)]+ 2H_2O \quad (1^{st}\text{event})$$

$$[Ho(acac)_3(H_2O)] \xrightarrow{137.3\,^{\circ}C} [Ho(acac)_3] + H_2O \quad (2^{nd}\text{event})$$

$$[Ho(acac)_3] \xrightarrow{239.5\,^{\circ}C} [Ho(acac)(CH_3COO)_2] + 2C_3H_4 \quad (3^{rd}\text{ event})$$

$$[Ho(acac)(CH_3COO)_2] \xrightarrow{282\,^{\circ}C} [Ho(CH_3COO)_3] + C_3H_4 \quad (4^{th}\text{ event})$$

$$2[Ho(CH_3COO)_3] \xrightarrow{400\,^{\circ}C} [Ho_2(CH_3COO)_4(CO_3)] \quad (5^{th}\text{ event})$$

$$[Ho_2(CH_3COO)_4(CO_3)] \xrightarrow{600\,^{\circ}C} Ho_2(CO_3)_3 \quad (6^{th}\text{ event})$$

The HoAcAc DTA curve (Figure 4(B)) displays a thermal event (96.3 ^{O}C) between temperatures of release of superficial and inner sphere water molecules of the complex. They can be related to the crystal structure rearrangement to form a dehydrated species. Three other endothermic events occur in temperatures covering the formation of the intermediate $Ho_2(CH_3COO)_4(CO_3)$.

Raw PDLLA has ester bonds in terminal and inner parts of its polymer chains because of different of hydrolysis rates (Shih 1995). Based on this, it is proposed that a thermal destruction of polyester (Figure 5(A)) may involve two events. The first, at 320.2 °C, would be a mass loss coming from terminal esters more exposed to heat transfer, and the one at 326.8 °C would represent the same process involving innermost groups. At 383.9 °C, total degradation of material is observed. The PDLLA DTA curve (Figure 5(B)) shows a thermal event at about 103.0 °C, which is assigned as melting of amorphous PDLLA (Kaitia *et al*. 1996). The DTA curve shows an endothermic event at 306.2 °C and an exothermic one at 326.5 °C, caused by (1) crystallinity change of the polymer due to heating and (2) subsequent thermal degradation of the polymer beginning from the outer esters bonds and followed by inner ones.

FIGURE 5

The MS-PDLLA TGA curve (Figure 5(C)), presents the first mass loss at 79 °C, which is attributed to the release of residual organic solvent and water from the microspheres. The DTA curve (Figure 5(D)) showed thermal events at 266.2 ^{O}C and 296.2 ^{O}C, which revealed changes in the intermolecular and intramolecular interactions of the melted polyester prior to its thermal decomposition. The TGA curve of the raw polymer (Figure 5(A)) contained two small mass losses at 320.2 °C and 326.8 °C, attributed to two kinds of degradation of the polyester. However, the MS-PDLLA curve showed only one mass loss at a slightly higher temperature (333.7 °C). This might indicate that melted MS-PDLLA is more disordered than the raw polymers.

MS-PDLLA-HoAcAc began to degrade in lower temperatures than MS-PDLLA and raw PDLLA, (data not shown), possibly because the first material is less crystalline. The first mass loss at 81.70 °C is assigned to loss of residual organic solvent and hydration water molecules. The second weight loss of 63.41% at 197.3 °C is ascribed to degradation of polyester chains. The third mass loss of 8.24%, at 422.4 °C represented full decomposition.

The DTA curve of MS-PDLLA-HoAcAc (data not shown) showed that the polymer melting temperature (108.4 °C) was slightly higher than the MS-PDLLA one (103.1 °C), which might indicate an increase in degree of crystallinity with the presence of $Ho(AcAc)_3$. There were two thermal events; an endothermic one at 231.3 °C, and an exothermic one at 256.2 °C. They are proposed to be related to structural changes between the polymer and HoAcAc along the thermal decomposition of the microspheres, as it can be observed in TGA curve. At 370 °C, the endothermic event was very similar to the one seen in raw $Ho(AcAc)_3$ hence it is assigned to a crystalline rearrangement of intermediates.

Release of HoAcAc from MS-PDLLA-HoAcAc in phosphate buffer saline (pH 7.40)

The clinical application of holmium acetylacetonate microspheres (MS-PDLLA-HoAcAc) for the intratumoral radionuclide treatment of solid malignancies requires a thorough understanding of their stability. Preliminary studies of those were conducted analyzing the potential release of the holmium complex in a solution that mimics the physiological environment (Bult *et al*. 2012). The release of the holmium complex in phosphate buffer was performed using a calibration curve (Intensity (c/s) x Ho^{3+}

concentration (ppm)) to a reference solution of holmium III chloride, which presented the Curve Equation: $y = 9493.7 x + 1251.8$ and Correlation Coefficient: $R^2 = 0.998881$.

The sample before and after 25 kGy gamma irradiation seemed to present a negative value for Ho^{3+} in the solution, as described in Table 2. The negative value was assigned to the sodium ion contamination in raw products used to prepare the buffer and the contamination has unknown source.

TABLE 2

Conclusion

The presence of the HoAcAc in microspheres was confirmed by EDS analysis, fluorescence techniques and SEM images. HoAcAc was not free and even the sterilization of microspheres by 25 kGy gamma irradiation dose did not lead to HoAcAc leakage. Thus, we present MS-PDLLA-HoAcAc as a promising system for brachytherapy purposes. Nevertheless, prior to their use their stability in biofluids should be assessed and toxicology tests must be carried out.

Acknowledgments

We would like to thank for the financial support given by:
Radiopharmacy Department (DIRF/IPEN/CNEN);
Brazilian Nacional Research Council (CNPq), Processes: **550598/2010-3;310227/2010-0; 381405/2011-7; 111795/2011-7.**
In memoriam, Dr. José Roberto Martinelli, IPEN.

References

Avinc O, Khoddami A. Overview of poly(lactic acid) (PLA) fibre. Part I: production, properties, performance, environmental impact, and end-use applications of poly(lactic acid) fibres. Fibre Chem, 2009;41:391-401.

Bakker RC, Lam MGEH, Nimwegen SAV, Rosenberg AJWP, Es RJJV, Nijsen FW. Intratumoral treatment with radioactive beta-emitting microparticles: a systematic. J Radiat Oncol, 2017; 6:323-41.

Bult W, Leeuw H, Steinebach OM, J. van der Bom M, Wolterbeek HT, Heeren RMA, Bakker CJG, van het Schip AD, Hennink WE, Nijsen JFW. Radioactive holmium acetylacetonate microspheres for interstitial microbrachytherapy: an in vitro and in vivo stability study. Pharm Res, 2012;29:827–36.

Bunzli J-C, Piguet C. Taking advantage of luminescent lanthanide ions. Chem Soc Rev, 2005;34:1048-77.

Cheng Y, Deng S, Chen P, Ruan R. Poly lactic acid (PLA) synthesis and modifications: a review. Front Chem China, 2009;4:259-64.

Colthulp NB, Day LH, Wiberley SE. Introduction to Infrared and Raman Spectroscopy. 1990 3ª ed, Academic Press.

Costa RF, de Azevedo MBM, Nascimento N, Sene FF, Martinelli J R, Osso Jr JA. International Nuclear Atlantic Conference - INAC 2009; ABEN ISBN: 978-85-99141-03-8.

Cui W, Li X, Zhou S, Weng J. In situ growth of hydroxyapatite within electrospun poly(DL-lactide) fibers. J Biomed Mater Res A, 2007;82:831-41.

Dhanasekahan R, Limaye A, Cabrera R. Hepatocellular carcinoma: current trends in worldwide epidemiology, risk factors, diagnosis, and therapeutics. Hepat Med, 2012;4:19-37.

Diaz-Acosta I, Baker J, Cordes W, Pulay P. Calculated and Experimental Geometries and Infrared Spectra of Metal Tris-Acetylacetonates: Vibrational Spectroscopy as a Probe of Molecular Structure for Ionic Complexes. Part I J Phys Chem A, 2001;105:238-44.

Dubois P, Narayan R. Biodegradable compositions by reactive processing of aliphatic polyester/polysaccharide blends. Macromol Symp, 2003;198:233-43.

Frank MM, Fries LF. The role of complement in inflammation and phagocytosis. Immunology Today. 1991;12:322-26.

Garlotta D. A Literature review of poly(lactic acid). J Polym Environm, 2001;9:63-84.

Gasparini G, Kosvintsev SR, Stillwell MT, Holdich RG. Preparation and characterization of PLGA particles for subcutaneous controlled drug release by membrane emulsification. Colloid Surface B, 2008;61(2):199-207..

Ginty PJ, Whitaker MJ, Shakesheff KM, Howdle SM. Drug delivery goes supercritical. Mater Today, 2005;8:42-8.

Giunchedi P, Conti B, Genta I, Conte U, Puglisi G. Emulsion spray-drying for the preparation of albumin-loaded PLGA microspheres. Drug Dev. Ind. Pharm , 2001;27(7):745-50.

Han B, Wang X, Gao X, Liu J, Liang F, Qu X, Yang Z. Synthesis and characterization of biodegradable microcapsules for the controlled delivery of calcium hydroxide. J Biomed Mater Res B Appl Biomater, 2011,99:120-6.

Han S, Zhang X, Li M. Progress in research and application of PLGA embolic microspheres, Frontiers in Bioscience, 2016,4:230-43.

Helen W, Gough JE. Cell viability, proliferation and extracellular matrix production of human annulus fibrosus cells cultured within PDLLA/Bioglass composite foam scaffolds *in vitro*. Acta Biomaterial, 2008;4:230-43.

Hu Y-S, Zhang ZP, Song D, Bai DR, Wang Y-M. Preparation and properties of high strength rods from L- and D,L-lactide copolymer. Chinese J Polym Sci, 2001;19:351-7.

Hussein GAM, Ismail HM. Characterization of lanthanium oxide formed as a final decomposition product of lanthaniumacetylacetonate: thermoanalytical, spectroscopic and microscopic studies. Powder Technol, 1995;84:185-90.

Hussein GAM. Rare earth metal oxides: formation, characterization and catalytic activity. Thermoanalytical and applied pyrolysis review. J Anal Appl Pypol, 1996;37:111-49.

Ikada Y, Tsuji H. Biodegradable polyesters for medical and ecological applications. Macromol Rapid Commun, 2000;21:117-32.

Jacobsen S, Degée P, Fritz HG. Polylactide (PLA)-a new way of production. Polym Eng Sci, 1999;39:1311-9.

Jain RA. The manufacturing techniques of various drug loaded biodegradable poly (lactide-co-glycolide)(PLGA) devices. Biomaterials, 2000;21(23):2475-90.

Jain S, Reddy MM, Mohanty AK, Misra M, Ghosh AK. A New Biodegradable flexible composite sheet from poly(lactic acid)/poly(ε-caprolactone) blends and micro-Talc. Macromol Mater Eng, 2010; 295:750-62.

Jung J, Perrut M. Particle design using supercritical fluids: literature and patent survey. J Supercrit Fluid 2001, 20:179-219.

Kaitia X, Kozluca A, Denba EB, Piskin E. Poly (D,L – Lactic Acid) Homopolymers: Synthesis and Characterization. Tr J of Chemistry, 1996;43-3.

Kim JH, Lee JT, Kim EK, Won JY, Kim M-J, Lee JD, Hong SJ. Percutaneous sclerotherapy of renal cysts with a beta-emitting radionuclide, Holmium-166-chitosan complex. Korean J Radiol, 2004;5:128-33.

Koojiman H, Nijsen JF, Spek AL, Van Het Schip AD. Diaquatris(pentane-2,4-dionato-O, O') holmium (III) monohydrate and diaquatris(pentane-2,4-dionato-O,O') holmium (III) 4-hydroxypentan-2-one solvate dehydrate. Acta Crystallogr C, 2000;56:156-8.

Kricheldorf HR. Syntheses and application of polylactides. Chemosphere, 2001;43:49-54.

Leal CR, Martinez DST, Espósito AR, MásI BA, Moraes ACM, Alves OL, Duek EAR. Caracterização e avaliação in vitro de nanocompósitos de poli (L-ácido lático) e nanotubos de carbono de paredes múltiplas purificados. Quim Nova, 2015;38:1153-61.

Lin YM, Boccaccini AR, Polak JM, Bishop AE. Biocompatibility of poly-DL-lactic acid (PDLLA) for lung tissue engineering. J Biomater App, 2006;21:109-18.

Lliakis G. The role of DNA double strand breaks in ionizing radiation-induced killing of eukaryotic cells. BioEssays. 1991;13:641-48.

Mansur HS, Sadahir, CM, Souza AN, Mansur AAP. FTIR spectroscopy characterization of poly (vinyl alcohol) hydrogel with different hydrolysis degree and chemically crosslinked with glutaraldehyde, Mat Sci Eng C Biomim, 2008;28:539-48.

Milenic DE, Brady ED, Brechbiel, MW. Antibody targeted radiation cancer therapy. Nat Rev Drug Discov, 2004;3:488-99.

Mi F, Lin Y, Wu Y, Shyu S, Tsai Y. Chitin/PLGA blend microspheres as a biodegradable drug-delivery system: phase-separation, degradation and release behavior. Biomaterials, 2002;23(15):3257-67.

Mumper RJ, Jay M. Biodegradable radiotherapeutic polyester microspheres: optimization and in vitro/in-vivo evaluation. J Control Release, 1991;18:193-204.

Nijsen JFW, Zonnenberg BA, Woittiez JR, Rook DW, Swildens-van Woudenberg IA, Van Rijk PP, Van het Schip AD. Effects of preparation and neutron activation techniques, Eur J Nucl Med, 1999;26:699-704.

Nijsen JFW, van Steenbergen M J, Kooijiman H, Talsma H, Kroon-Batenburg LMJ; van de Weert M, van Rijk PP, de Witte A, van het Schip AD, Hennink W E. Characterization of poly(L-acid lactic) microspheres loaded with holmium acetylacetonate loaded. Biomaterials, 2001;22:3073-81.

Nijsen JFW, van het Schip AD, van Steenbergen MJ, Zielhuis SW, Kroon-Batenburg LMJ, van de Weert M, van Rijk PP Hennink WE. Influence of neutron irradiation on holmium acetylacetonate loaded poly(L-lactic acid) microspheres. Biomaterials, 2002;23:1831-39.

Owens DE, Peppas NA. Opsonization, biodistribution, and pharmacokinetics of polymeric nanoparticles. Int J Pharm, 2006;307:93-102.

Parhizkar M, Reardon PJT, Knowles JC, Browning RJ, Stride E, Barbara PR, Harker AH, Edirisinghe M. Electrohydrodynamic encapsulation of cisplatin in poly(lactic-co-glycolic acid) nanoparticles for controlled drug delivery. Nanomedicine: NBM, 2016;12:1919-29.

Piovan TPG, Pires G, de Lira RA, Geraldes AN, Nascimento N, de Melo VHS, Kodama Y, de Azevedo MBM. International Nuclear Atlantic Conference - INAC 2011; ABEN ISBN: 978-85-99141-04-5.

Rajendran JG, Eary JF, Bensinger W, Durack LD, Vernon C, Fritzberg A. High-dose 166 Ho-DOTMP in myeloablative treatment of multiple myeloma: pharmacokinetics, biodistribution, and absorbed dose estimation. J Nucl Med, 2002;43:1383-90.

Reardon PJT, Parhizkar , Harker AH, Browning RJ, Vassileva V, Stride E, Pedley, RB, Edirisinghe, Knowles, JC. Electrodynamic fabrication of core-shell PLGA nanoparticles with controlled release of cisplatin for enhanced cancer treatment. Int J Nanomedicine, 2017;12:3913-26.

Rosca ID, Fumio W, Motohiro U. Microparticle formation and its mechanism in single and double emulsion solvent evaporation. J control Release, 2004;99(2):271-80.

Sato K. Radiation sterilization of medical products. Radioisotopes, 1983;32:431-9.

Seyednejad H, Ghassemi AH, van Nostrum CF, Vermonden T, Hennink, WE.Functional aliphatic polyesters for biomedical and pharmaceutical applications. J Control Release, 2011;152:168-76.

Shams T, Parhizkar M, Illangakoon UE, Orlu M,Edirisinghe M.Core/shell microencapsulation of indomethacin/paracetamol by co-axial electrohydrodynamic atomization. Mater Des, 2017;136:204-13.

Shih C. Chain-end scission in acid catalyzed hydrolysis of poly(D,L-lactide) in solution. J Control Release, 1995;34:9-15.

Shiga K, Muramatsu N, Kondo T. Preparation of Poly (D, L-lactide) and Copoly (lactide-glycolide) Microspheres of Uniform Size. J Pharm Pharmac, 1996; 48(9):891-5.

Smits MLJ, Nijsen JFW, van den Bosch MAAJ, Lam MGEH, Vente MAD, Huijbregts JE, van het Schip AD, Elschot M, Bult W, de Jong HWAM, Meulenhoff PCW, Zonnenberg BA. Holmium-166 radioembolization for the treatment of patients with liver metastases: design of the phase I HEPAR trial. J Exp Clin Cancer Res, 2010;29:70:2-11.

Södergård A, Stolt M. Properties of lactic acid based polymers and their correlation with composition. Prog Polym Sci, 2002;27:1123-63.

Speenwoolde JH, Nijsen JF, Bartel LW, Zielhus SW, van het Schip AD, Bakker CJ. Internal biodistribution of holmium-loaded microspheres in animal models. Magn Reson Med, 2004;53:76-84.

Spinu M, Jackson C, Keating MY, Gardner KH. Material design in poly(lactic acid) systems: block copolymers, star homo- and copolymers, and stereocomplexes. J Macromol Sci Pure Appl Chem A, 1996;33:1497-1530.

Thunus L, Lejeune R. Overview of transition metal and lanthanide complexes as diagnostics tools. Coord Chem Rev, 1999;184:125-55

Tuner JH, Claringbold PG, Kelmp PBF, Cameron PJ, Martindale AA, Glancy RJ, Norman PE, Hetherington EL, Najdovski L, Lambrecht RM. 166-Ho microsphere liver radiotherapy: a pre-clinical SPECT dosimetry study in the pig. Nucl Med Comm, 1994;15:545-53.

Van Es RJJ, Nijsen JFW, van het Schip AD, Dullens HFJ, Slootweg PJ, Koole R. Intra-arterial embolization of head-and-neck cancer with radioactive holmium-166 poly(L-lactic acid) microspheres: an experimental study in rabbits. Int J Oral Maxillofac Surg, 2001;30:407-13.

Vente MA, Nijsen JF, Wit TC, Seenwoolde JH, Krijger GC, Seevinck PR, Huisman A, Zonnenberg BA, van den Ingh TSGAM, van het Schip AD. Clinical effects of transcatheter hepatic arterial embolization with holmium-166 poly(L-lactic acid) microspheres in healthy pigs. Eur J Nucl Med Mol Imaging, 2008; 35:1259-71.

Xu H, Yan Y, Li S. PDLLA/chondroitin sulfate/chitosan/NFG conduits for peripheral nerve regeneration. Biomaterials, 2011;32:4506-16.

Williams JR, Clifford AA, Al-Saidi SHR. Supercritical fluids and their applications in biotechnology and related areas. Mol Biotechnol, 2002;22:263-86.

Yang YY, Chi HH, Chung TS. Effect of preparation temperature on the characteristics and release profiles of PLGA microspheres containing protein fabricated by double emulsion solvent extraction/evaporation method. J Control Release 2000;69(1):81-96.

Zielhuis SW, Nijsen JFW, de Roos R, Krijger GC, van Rijk PP, Hennink WE, van het Schip AD. Production of GMP-grade radioactive holmium loaded poly(L-lactic acid) microspheres for clinical application. Int J Pharm, 2006;311:69-74.

Zielhuis SW, Nijsen JFW, Seenwoolde JH, Bakker CJG, Krijger GC, Dullens HF, Zonnenberg BA, van Rijk PP, Hennink WE, van het Schip AD. Long-term toxicity of holmium loaded poly(L-lactic acid) microspheres in rats. Biomaterials, 2007;28:4591-99.

LEGENDS

Figure 1. Scanning Electron Microscopy (SEM) images of (A) PDLLA microspheres (MS-PDLLA) and (B) HoAcAc loaded PDLLA microspheres (MS-PDLLA-HoAcAc) with magnification of 1000x. SEM images of (C) MS-PDLLA-HoAcAc before irradiation and (D) after a 25 kGy gamma rays dose. No morphological change or HoAcAc leakage was observed after the irradiation.

Figure 2. (A) Optical microscope fluorescence image of HoAcAc loaded PDLLA microspheres (MS-PDLLA-HoAcAc) (magnification 20x); (B) Scanning Electron Microscopy (SEM) image of HoAcAc, raw crystals (magnification 500x). (C) Energy dispersive X-ray spectroscopy (EDS) spectra of the MS-PDLLA-HoAcAc displaying typical holmium peaks, which confirms the HoAcAc loading inside the microspheres.

Figure 3. Fourier Transform Infrared Spectroscopy (FTIR) spectra of HoAcAc, PDLLA microspheres (MS-PDLLA), HoAcAc loaded PDLLA microspheres (MS-PDLLA-HoAcAc) and poly(vinyl alcohol) (PVA).

Figure 4. (A) Thermogravimetric analysis (TGA) curve of HoAcAc and its first derivative showing consecutive thermal events which correspond to a multistep propyne loss leading to $Ho_2(CO_3)_3$ as the end product; (B) Differential thermogravimetric analysis (DTA) and TGA curves of HoAcAc.

Figure 5. (A) Thermogravimetric Analysis (TGA) curve and its first derivative and (B) DTA and TGA curves of raw PDLLA. A change in polymer crystallinity followed by destruction of outer ester bonds and then inner ester bonds is proposed. (C) TGA and its

first derivate curve and (D) Differential Thermogravimetric Analysis (DTA) and TGA curves of PDLLA microspheres (MS-PDLLA). Only one mass loss corresponding to polymer thermal degradation is observed, indicating a higher degree of disorder.

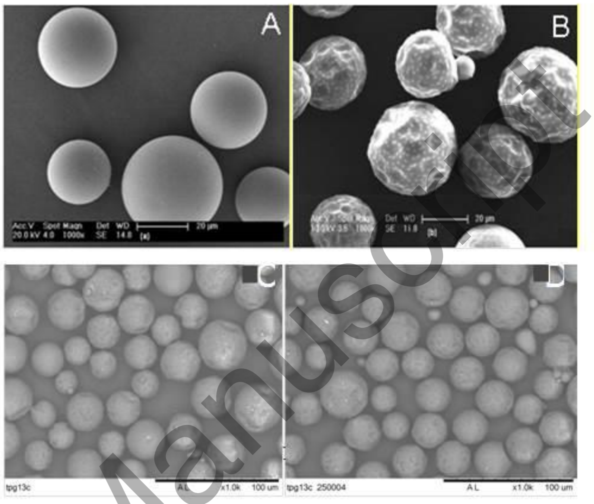

Fig. 1

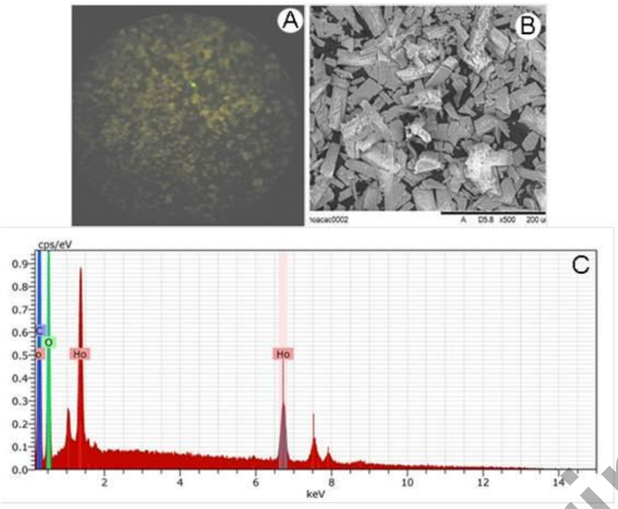
A
B
hoacac0002
A D5.8 x500 200 um
C
cps/eV
0.9
0.8
0.7
0.6
0.5
0.4
0.3
0.2
0.1
0.0
C
O
O
Ho
Ho
2
4
6
8
10
12
14
keV

Fig. 2

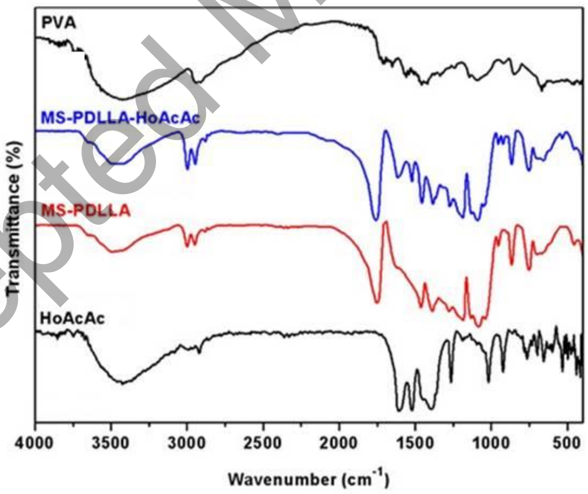
PVA
MS-PDLLA-HoAcAc
MS-PDLLA
HoAcAc
Transmittance (%)
4000
3500
3000
2500
2000
1500
1000
500
Wavenumber (cm-1)

Fig. 3

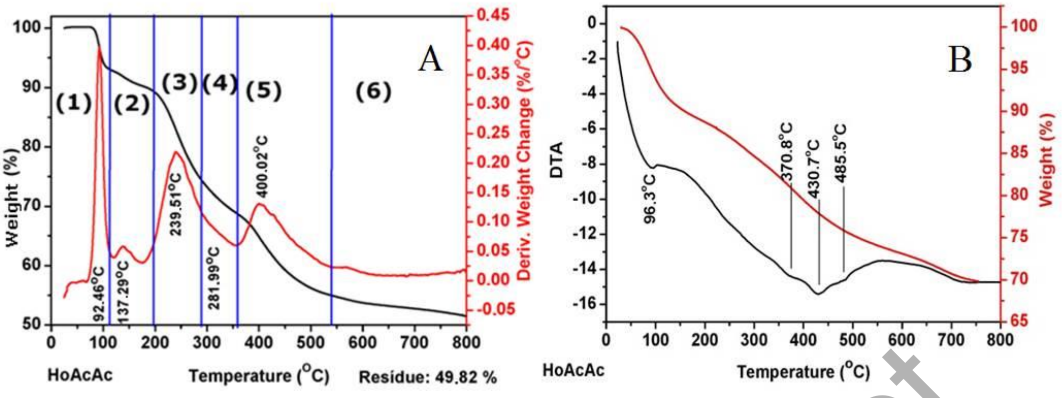
A
B
(1)
(2)
(3)
(4)
(5)
(6)
Weight (%)
100
90
80
70
60
50
Deriv. Weight Change (%/°C)
0.45
0.40
0.35
0.30
0.25
0.20
0.15
0.10
0.05
0.00
-0.05
92.46°C
137.29°C
239.51°C
281.99°C
400.02°C
0
100
200
300
400
500
600
700
800
HoAcAc
Temperature (°C)
Residue: 49.82 %
DTA
0
-2
-4
-6
-8
-10
-12
-14
-16
Weight (%)
100
95
90
85
80
75
70
65
96.3°C
370.8°C
430.7°C
485.5°C
HoAcAc
Temperature (°C)

Fig. 4

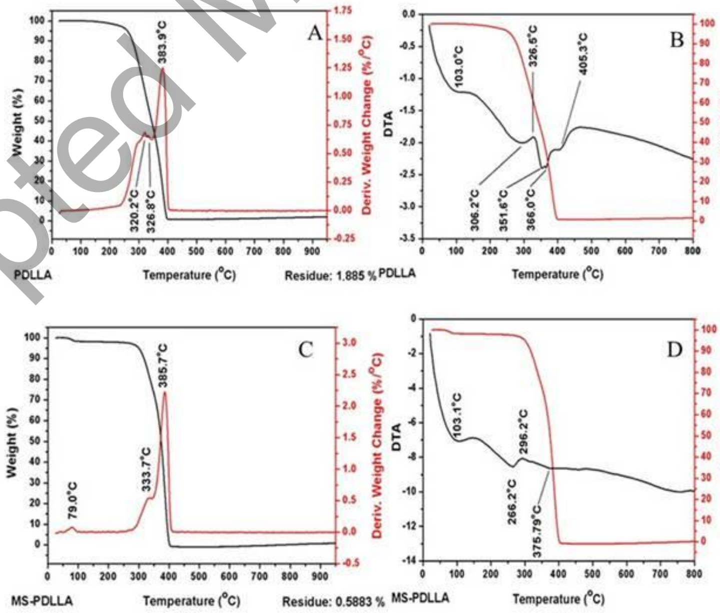
A
Weight (%)
Deriv. Weight Change (%/°C)
1.75
1.50
1.25
1.00
0.75
0.50
0.25
0.00
-0.25
383.9°C
320.2°C
326.8°C
PDLLA
Temperature (°C)
Residue: 1.885 %
B
DTA
0.0
-0.5
-1.0
-1.5
-2.0
-2.5
-3.0
-3.5
Weight (%)
103.0°C
326.5°C
405.3°C
306.2°C
351.6°C
366.0°C
PDLLA
Temperature (°C)
C
Weight (%)
Deriv. Weight Change (%/°C)
3.0
2.5
2.0
1.5
1.0
0.5
0.0
-0.5
385.7°C
333.7°C
79.0°C
MS-PDLLA
Temperature (°C)
Residue: 0.5883 %
D
DTA
0
-2
-4
-6
-8
-10
-12
-14
Weight (%)
103.1°C
296.2°C
266.2°C
375.79°C
MS-PDLLA
Temperature (°C)

Fig. 5

Table 1. Assignments to normal modes of HoAcAc, emulsifier agent and the prepared microspheres.

HoAcAc	**PVA**	**MS-PDLLA**	**MS-PDLLA-HoAcAc**	**Assignment**
3421	3421	3490	3437	ν(O-H)
2997		2997	2997	ν(C-H)
2966	2943	2947	2497	ν(C-H)
2924	2912			ν(CH)
	1716	1755	1759	ν(C=O)
	1650			ν(C=C)
	1558	1627		ν(C=O)
1605			1612	ν(C=O)
1524			1524	ν(C=C)
1450 sh	1458	1462	1454	$\delta(CH_{op})$
	1438			$\delta(CH_{op})$
1396				ν(C=O)+ ν(C=C)
	1373	1389	1385	$\delta(CH_{op})$
	1350-1180			$\omega(CH_2)$
		1280	1273	ν_{ass}(C-C-O)
1265			1273	ν(C=O)+ ν(C-CH_3)
	1242			ν (HO-CCH_3)
		1188	1188	νa_{ss}(C-C-O)
	1145	1134	1126	$\nu(C\text{-}C\text{-}C)_{ip}+\rho(CH_3)$
	1095	1084	1088	ν(C-O)
		1041	1049	ν_{sym}(O-CH_2)
1018				$\rho(CH_3)$+ν(C=O)
		956	957	ν_{sym}(O-CH_2)
922			922	ν(C-CH_3)
		864	868	$\nu(C\text{-}C\text{-}C)_{ip}+\rho(CH_3)$
	848			$\nu(C\text{-}C\text{-}O)_{ip}$
764				π(C-H)
		752	756	ρ(C=O)
698				π(C-H)
	663	698	698	$\delta(C\text{-}OH)_{op}$
656				ν(C-CH_3)+ ν(Ho-O)
602				ω(C=O) enol
536			536	δ(O=C-CH_3)
494				ν(Ho-O)
474				ν(Ho-O)
		455	451	
424				δ(C=C-CH_3)

Abbreviations: sh = shoulder. op = out of phase, ip = in phase; ass = asymmetric; sym = symmetric; ν = stretching, δ = bending, ρ = rocking, ω = wagging.

Table 2. Intensity and Ho^{3+} concentration in phosphate buffer, pH 7.4, related to holmium III release.

Sample	Intensity (c/s)	Intensity (c/s)	Holmium III Concentration (ppm)
BLANK - phosphate buffer	9.865	-	-
MS-PDLLA-HoAcAc SI (11 days)	31.71	21.845	-0.129
MS-PDLLA-HoAcAc-25kGy SI (11 days)	7.964	-1.901	-0.132